Ionization and recombination rates of atomic oxygen in high-temperature air plasma flows

A. Bourdon, Y. Térésiak, and P. Vervisch
Université de Rouen, CNRS UMR No. 6614 CORIA, 76821 Mont Saint Aignan Cedex, France
(Received 4 December 1997)

A nonlinear time-dependent collisional-radiative model for atomic oxygen is presented. Effective ionization and three-body recombination rate coefficients are calculated for either optically thin or thick plasmas where $10^{18}\ \mathrm{m}^{-3} \leqslant n_e \leqslant 10^{21}\ \mathrm{m}^{-3}$ and $8000\ \mathrm{K} \leqslant T_e \leqslant 20\,000\ \mathrm{K}$. In order to implement these coefficients easily in plasma flow codes, simple analytical expressions are proposed. Significant discrepancies with existing literature values are pointed out and discussed. The time-dependent approach confirms the importance of a quasi-steady-state condition to derive meaningful rate coefficients. Therefore the relaxation time necessary for the system to reach a quasi-steady-state limits the validity of the rate coefficients determined in this study. In optically thick cases, this relaxation time in either recombining or ionizing plasmas depends weakly on the electron temperature but strongly increases as the electron number density decreases. In optically thin cases, it is more difficult to derive general results since the relaxation time depends on the electron temperature, on densities, but also on the initial distribution on atomic levels. [S1063-651X(98)08104-5]

PACS number(s): 52.20.−j, 31.70.Hq, 47.70.−n, 82.40.Ra

I. INTRODUCTION

Despite the large number of experimental and theoretical studies on high-temperature air chemistry, uncertainties remain on the accuracy of numerous reaction rates. In particular, the effective ionization and recombination rates of atoms are difficult to determine experimentally and then most available results have been derived from theoretical studies. However, a reaction such as $O^+ + 2e^- \leftrightarrow O + e^-$ results from numerous different elementary processes between the atomic levels of oxygen. Therefore, the accuracy of theoretical effective ionization and recombination rate coefficients depends on the choice of the atomic model and on the choice of the rate coefficients for the elementary processes. In our previous paper [1], referred to as paper I, a nonlinear collisional radiative model was developed for atomic nitrogen. In this paper, we propose to set up a collisional radiative model for atomic oxygen in order to determine effective ionization and recombination rate coefficients for $10^{18}\ \mathrm{m}^{-3} \leqslant n_e \leqslant 10^{21}\ \mathrm{m}^{-3}$ and $8000\ \mathrm{K} \leqslant T_e \leqslant 20\,000\ \mathrm{K}$. In an earlier study, Taylor and Ali [2] determined these rate coefficients for slightly different conditions: $10^{22}\ \mathrm{m}^{-3} \leqslant n_e \leqslant 10^{25}\ \mathrm{m}^{-3}$ and $1\ \mathrm{eV} \leqslant T_e \leqslant 3\ \mathrm{eV}$. Other previous collisional radiative models for oxygen have been devoted to the study of the population densities at the stationary state [3,4] and relaxation times [5]. Since the study of Taylor and Ali, numerous experiments and computations have been carried out to improve the accuracy of atomic cross sections and Einstein coefficients in oxygen. In this work, we have tried to determine the best possible coefficients available in the literature. The data critically compiled by Soon and Kunc [4] have been used with a few updates on e-O inelastic collisions [6] and on Einstein coefficients [7,8]. In this study, we consider a spatially uniform and electrically neutral plasma. We assume that the distributions of energies of particles are Maxwellian and that the atom-atom and ion-atom inelastic collisions are negligible. The treatment of radiation is limited to either optically thin or optically thick cases.

Unfortunately, no experimental data are available on the effective ionization and recombination rates of atomic oxygen to compare with our results. In high-temperature air kinetic schemes used in plasma flow codes, different analytical expressions, whose accuracy is unknown, are proposed for these rate coefficients [9–11]. Therefore, this work is the opportunity to study the validity of these simple analytical expressions for the effective ionization and recombination rates of atomic oxygen. Furthermore, the time-dependent approach used in this paper allows us to follow the relaxation of atomic level populations and to study the validity of the quasi-steady-state hypothesis.

II. ATOMIC MODEL

In this work, forty coalesced energy levels of the neutral oxygen atom have been considered [12]. Their characteristics are given in Table I. As in the nitrogen atom, there is a large energy gap in the oxygen atom between the two first metastable levels ($2s^2 2p^4\ ^1D$ and $2s^2 2p^4\ ^1S$) and the other excited levels, which lie in a narrow region of energy. However, it is interesting to note that in the oxygen atom, the resonant level is only the fifth level, located 9.52 eV from the ground state. In their atomic model for oxygen, Soon and Kunc [4] considered only the first nine levels of our model. In this case, the last level lies 1.69 eV under the ionization limit. With our model, this energy gap is only of 0.124 eV. The influence of the atomic model on the results will be discussed in the following sections. In the electron temperature range of our study, we consider only the ground ionic term of O^+, $2s^2 2p^3\ ^4S$ (13.62 eV), which is taken as the ''core'' for all atoms. Processes involving O^- ions could *a priori* also influence the determination of the ionization and recombination rate coefficients. However, Soon and Kunc [13] showed that for $T_e \geqslant 8000\ \mathrm{K}$, the contribution of O^- ions to production of electrons, positive ions, and excited atoms is negligible. Therefore, in this study, the influence of O^- ions has been neglected.

TABLE I. Atomic level model.

Level index i	Configuration $1s^2+$	Energy E_i (eV)	Statistical weight g_i
1	$2s^2 2p^4(^3P)$	0.000	9
2	$2s^2 2p^4(^1D)$	1.970	5
3	$2s^2 2p^4(^1S)$	4.190	1
4	$2s^2 2p^3 3s(^5S^o)$	9.150	5
5	$2s^2 2p^3 3s(^3S^o)$	9.520	3
6	$2s^2 2p^3 3p(^5P)$	10.740	15
7	$2s^2 2p^3 3p(^3P)$	10.990	9
8	$2s^2 2p^3 4s(^5S^o)$	11.840	5
9	$2s^2 2p^3 4s(^3S^o)$	11.930	3
10	$2s^2 2p^3 3d(^5D^o)$	12.090	25
11	$2s^2 2p^3 3d(^3D^o)$	12.100	15
12	$2s^2 2p^3 4p(^5P)$	12.300	15
13	$2s^2 2p^3 4p(^3P)$	12.370	9
14	$2s^2 2p^3 3s'(^3D^o)$	12.550	15
15	$2s^2 2p^3 5s(^5S^o)$	12.670	5
16	$2s^2 2p^3 5s(^3S^o)$	12.710	3
17	$2s^2 2p^3 3s'(^1D^o)$	12.740	5
18	$2s^2 2p^3 4d(^5D^o)$	12.760	25
19	$2s^2 2p^3 4d(^3D^o)$	12.770	15
20	$2s^2 2p^3 4f(^5F,^3F)$	12.780	56
21	$2s^2 2p^3 5p(^5P)$	12.860	15
22	$2s^2 2p^3 5p(^3P)$	12.890	9
23	$2s^2 2p^3 6s(^5S^o)$	13.030	5
24	$2s^2 2p^3 6s(^3S^o)$	13.050	3
25	$2s^2 2p^3 5d(^5D^o,^3D^o)$	13.080	40
26	$2s^2 2p^3 5f(^5F,^3F)$	13.087	56
27	$2s^2 2p^3 6p(^5P)$	13.130	15
28	$2s^2 2p^3 6p(^3P)$	13.140	9
29	$2s^2 2p^3 7s(^5S^o)$	13.220	5
30	$2s^2 2p^3 7s(^3S^o)$	13.230	3
31	$2s^2 2p^3[6d(^5D^o,^3D^o), +6f(^5F,^3F) +6g(^5G^o,^3G^o)]$	13.250	168
32	$2s^2 2p^3 8s(^5S^o)$	13.330	5
33	$2s^2 2p^3 8s(^3S^o)$	13.340	3
34	$2s^2 2p^3[7d(^3D^o,^5D^o) +7d(^5F,^3F,)]$	13.353	96
35	$2s^2 2p^3 9s(^3S^o)$	13.412	3
36	$2s^2 2p^3 8d(^5D^o,^3D^o)$	13.418	40
37	$2s^2 2p^3 10s(^3S^o)$	13.459	3
38	$2s^2 2p^3 9d(^3D^o)$	13.464	15
39	$2s^2 2p^3 11s(^3S^o)$	13.493	3
40	$2s^2 2p^3 10d(^3D^o)$	13.496	15
41 (O^+ ion)	$2s^2 2p^3(^4S^o)$	13.620	4

III. ELEMENTARY RATE COEFFICIENTS

In a uniform plasma, the evolution of the population density of an excited atomic level i is due to different elementary processes

$$O_i + e^- \rightleftharpoons O_j + e^- \quad \text{for } i<j \quad [C_{ij}, C_{ji}], \tag{1}$$

where C_{ij} ($m^3\,s^{-1}$) and C_{ji} ($m^3\,s^{-1}$) are, respectively, the electron-impact excitation rate coefficient for the transition from the level i to the level j and its inverse deexcitation rate coefficient;

$$O_i + e^- \rightleftharpoons O^+ + 2e^- \quad [\beta_{ic}, \beta_{ci}], \tag{2}$$

where β_{ic} ($m^3\,s^{-1}$) and β_{ci} ($m^6\,s^{-1}$) are, respectively, the electron impact ionization rate coefficient from the level i and the three-body recombination rate coefficient on the level i;

$$O_j \rightarrow O_i + h\nu \quad \text{for } i<j \quad [A_{ji}], \tag{3}$$

where A_{ji} (s^{-1}) is the transition probability (Einstein coefficient) from the level j to the level i; and

$$O^+ + e^- \rightarrow O_i + h\nu \quad [\alpha_i^{RR}, \alpha_i^{RD}], \tag{4}$$

where α_i^{RR} ($m^3\,s^{-1}$) and α_i^{RD} ($m^3\,s^{-1}$) are, respectively, the radiative and dielectronic recombination rate coefficients on the level i. Dielectronic recombination is the result of a two-stage process:

$$O^+ + e^- \rightarrow O^* \rightarrow O_i + h\nu, \tag{5}$$

where O* represents an autoionizing state of the O atom.

A. Electron-impact excitation and deexcitation rate coefficients

Recently, reliable measurements of cross sections for several electron-impact excitation transitions have been carried out. For the $1 \rightarrow j \leqslant 7$ transitions, the cross sections measured by Doering and Gulcicek [14–17] have been used in agreement with the discussion of Soon and Kunc [4]. For the $1 \rightarrow 2$ transition, it is interesting to note that the shape and magnitude of the cross section have been confirmed recently by Doering [6]. For the $1 \rightarrow 9 \leqslant j \leqslant 19$ transitions, the cross sections reviewed by Laher and Gilmore [18] have been used. For all the other transitions, excitation cross sections have to be determined theoretically. For the $2 \rightarrow 3$ transition, the excitation cross section calculated by Thomas and Nesbet [19] has been used. This result is more recent and seems to be more reliable than the cross section determined earlier by Henry, Burke, and Sinfailam [20] and used by Soon and Kunc. For all the other transitions between levels, the energy of which is less than or equal to 11.93 eV, we have used the formalism developed by Sobelman, Vainshtein, and Yukov [21]. For ''difficult'' transitions (i.e., involving two atomic electrons), a binary-encounter approximation is used. All details are given in the paper of Soon and Kunc [4]. For atomic levels close to the continuum, all atoms are almost hydrogenic. Therefore, the formalism initially developed for hydrogen by Gryzinski [22] is used for these levels, and is no doubt more adapted than the Vainshtein formalism.

As discussed in Paper I, the use of two different theoretical approaches results in abrupt changes in the elementary rate coefficient values for intermediate transitions. In order to eliminate this anomaly, we introduce, in the same way, a correction factor such that elementary rate coefficient values vary smoothly from one model to the other. Discrepancies on the effective ionization and recombination rate values due to this correction remain within a factor of 2.

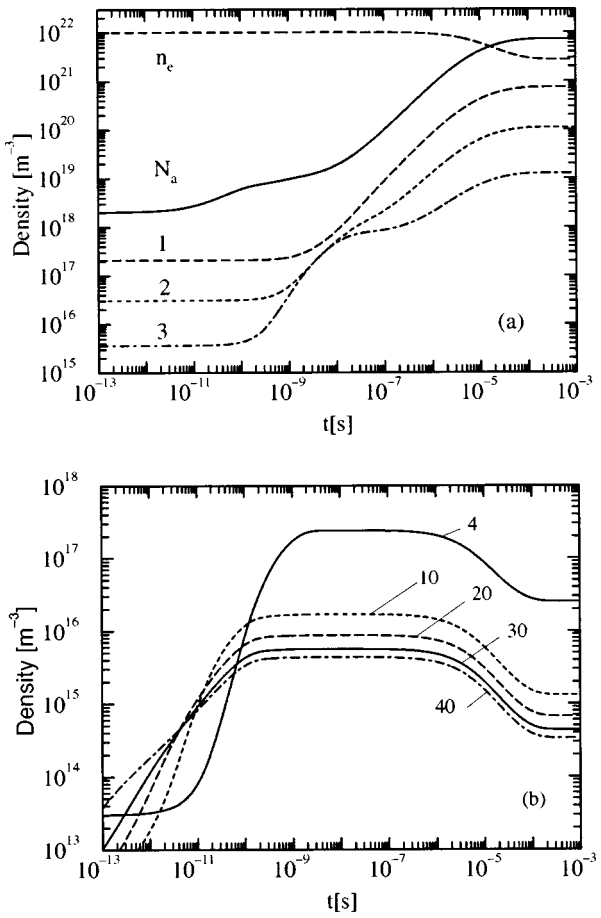

FIG. 1. (a),(b) Temporal evolution of densities for an initial recombining situation: at $t=0$ s, $T_e=12\,000$ K, $n_e=10^{20}$ m^{-3}, and $b_i=N_i/N_i^*=10^{-4}$, where N_i^* is the Saha density of level i. All elementary processes are taken into account, and the plasma is considered to be optically thin. Numbers denote atomic level numbers. Atomic level population densities are divided by their statistical weights.

B. Electron-impact ionization and three-body recombination rate coefficients

For the ground state and the two lowest excited levels, the models retained by Soon and Kunc [4] are used. For the other atomic levels, we have used the classical model approximation derived by Gryzinski and Kunc [23].

C. Spontaneous emission

For excited levels the energy of which is less than or equal to 11.93 eV, the transitions and the Einstein coefficients reviewed by Soon and Kunc are used. However, for the $5\rightarrow1$ and $9\rightarrow1$ transitions, the Einstein coefficients determined recently by, respectively, Biémont and Zeippen [7], and Bhatia and Kastner [8] have been used. For transitions issuing from levels lying higher than 11.93 eV, the best possible Einstein coefficients available in the literature have been used [8,24–27].

D. Radiative and dielectronic recombinations

The analytical expressions proposed by Nussbaumer and Storey [28] are used to calculate the dielectronic recombination coefficients for the effective (direct plus cascade) transitions to the terminating levels $i=1$ and 4. The total dielectronic recombination rate is

$$\alpha^{\mathrm{RD}}=\sum_{i=1,4}\alpha_i^{\mathrm{RD}}. \tag{6}$$

As in nitrogen, radiative recombination coefficients are significant only for the effective transitions to the three first atomic levels. Using the same approach as Soon and Kunc [4], we have calculated and fitted the associated total radiative recombination rate, and obtained

$$\alpha^{\mathrm{RR}}=\sum_{i=1}^{3}\alpha_i^{\mathrm{RR}}=2.12\times10^{-18}T_e^{-0.29}\ \mathrm{m^3\ s^{-1}}. \tag{7}$$

IV. MASTER EQUATIONS

Taking into account the different elementary processes mentioned above, the rate equations for the production of an excited atom on the level i can be written as

$$\frac{dN_i}{dt}=\dot{N}_i=\sum_{j\neq i}n_eN_jC_{ji}+\sum_{j>i}N_jA_{ji}\kappa_{ji}+n_eN^+[\alpha_i^{\mathrm{RR}}\kappa_i^{\mathrm{RR}}+\alpha_i^{\mathrm{RD}}\kappa_i^{\mathrm{RD}}+n_e\beta_{ci}]-N_i\left[\sum_{j\neq i}n_eC_{ij}+\sum_{k<i}A_{ik}\kappa_{ik}+n_e\beta_{ic}\right], \tag{8}$$

for $1\leqslant i\leqslant np$, where np is the total number of atomic levels, $n_e(\mathrm{m^{-3}})$ the electron number density, $N_i(\mathrm{m^{-3}})$ the population density of the atomic level i, and $N^+(\mathrm{m^{-3}})$ the number density of O^+. For the escape factors denoted by κ_{ij}, κ_i^{RR}, and κ_i^{RD}, respectively, for bound-bound, free-bound, and dielectronic radiation, we consider only the limit cases where they are equal either to 0 (optically thick plasma) or to 1 (optically thin plasma). The rate equation for the production of electrons is

$$\frac{dn_e}{dt}=\dot{n}_e=\sum_i n_eN_i\beta_{ic}-\sum_i n_e^2N^+\beta_{ci}-\sum_i n_eN^+[\alpha_i^{\mathrm{RR}}\kappa_i^{\mathrm{RR}}+\alpha_i^{\mathrm{RD}}\kappa_i^{\mathrm{RD}}]. \tag{9}$$

Finally, the electrical neutrality of the plasma imposes $n_e=N^+$. We denote $N_a=\Sigma N_i$, the total atomic density and $N_t=N_a+N^+$, the total particle density. The system of differential equations [Eqs. (8) and (9)] has been integrated numerically in using LSODE (Livermore Solver for Ordinary Differential Equations) [29]. In each set of calculations, T_e and N_t are constant.

V. RESULTS AND DISCUSSION

A. General behavior of time-dependent population densities

Figures 1(a) and 1(b) show the temporal evolution of the level populations for a typical recombining situation at $t=0$ s: $n_e=10^{22}$ m^{-3}, $T_e=12\,000$ K, and $b_i=N_i/N_i^*=10^{-4}$, where N_i^* is the Saha density of level i. The plasma is considered to be optically thin and all the elementary pro-

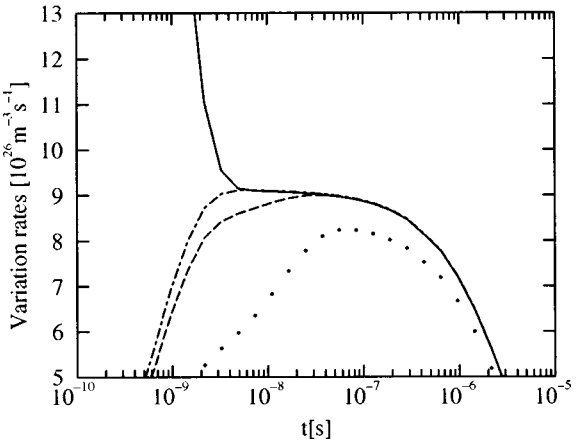

FIG. 2. Production rates of N_1, N_2, and N_3, and the depletion rate of n_e for the same initial recombining condition as in Fig. 1. Solid line: $|\dot{n}_e|$. Dotted line: $\dot{N}_1$. Dashed line: $\dot{N}_1+\dot{N}_2$. Dot-dashed line: $\dot{N}_1+\dot{N}_2+\dot{N}_3$.

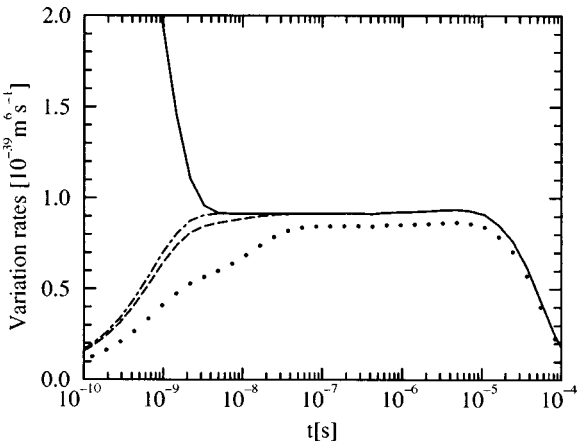

FIG. 3. Time variations of $|\dot{n}_e|/n_e^3$, $\dot{N}_1/n_e^3$, $(\dot{N}_1+\dot{N}_2)/n_e^3$, and $(\dot{N}_1+\dot{N}_2+\dot{N}_3)/n_e^3$ for the initial recombining condition of Fig. 1. Solid line: $|\dot{n}_e|/n_e^3$. Dotted line: $\dot{N}_1/n_e^3$. Dashed line: $(\dot{N}_1+\dot{N}_2)/n_e^3$. Dot-dashed line: $(\dot{N}_1+\dot{N}_2+\dot{N}_3)/n_e^3$.

cesses described above are considered. This example clearly puts forward that different time scales characterize the global relaxation process. For $t<10^{-10}$ s, in this example, N_1, N_2, N_3, and n_e vary only slightly in comparison to other excited state population densities. For 5×10^{-9} s$\leqslant t\leqslant10^{-6}$ s, the latter reach a plateau whereas N_1, N_2, N_3, and n_e vary significantly. Finally, all of the system tends toward a stationary state (reached at $t\simeq10^{-3}$ s in this example). As already observed in nitrogen, the populations of excited states at the plateau are very different from those at the stationary state. It is important to note that the general characteristics of the results are independent of the initial ionizing or recombining condition. Figure 2 shows the temporal evolutions of $|\dot{n}_e|$ and $\dot{N}_i$ for $1\leqslant i\leqslant3$. For $t\geqslant\tau_{\min}$ ($\tau_{\min}\simeq5\times10^{-9}$ s in this example), we have

$$\dot{N}_i\simeq0 \quad \text{for } i>3, \tag{10}$$

and then a quasi-steady-state condition of the form

$$|\dot{n}_e|=\sum_{i=1}^{3}\dot{N}_i, \tag{11}$$

can be written. This condition has been already established by Cacciatore and Capitelli [5] in oxygen and is the same as in nitrogen since both atoms have two low-lying levels. However, in oxygen, the fourth level is metastable too and then one could have expected to have for oxygen a quasi-steady-state (QSS) condition of the form

$$|\dot{n}_e|=\sum_{i=1}^{4}\dot{N}_i. \tag{12}$$

In the electron temperature and density range of our study, we have checked that Eq. (11) is the quasi-steady-state condition for oxygen.

B. General method to determine effective ionization and recombination rate coefficients

For the global reaction $O^+ + 2e^- \leftrightarrow O + e^-$, we define k_r, the effective three-body recombination rate coefficient, and k_i, the effective ionization rate coefficient, such that

$$\frac{dn_e}{dt}=\dot{n}_e=k_i n_e N_a - k_r n_e^3. \tag{13}$$

Both rate coefficients have to be time independent, but may depend on electron temperature and densities. To determine k_r, the method is to consider at $t=0$ s a recombining situation. In this case, in early times the first term on the right-hand side of Eq. (13) is far much smaller than the second one. Then, if k_r exists, there is a plateau in the temporal evolution of the ratio $|\dot{n}_e|/n_e^3$ and k_r is the value of this ratio at the plateau.

Conversely, to determine k_i, one has to consider at $t=0$ s an ionizing condition and to study the temporal evolution of the ratio $\dot{n}_e/(n_e N_a)$. k_i is the value of this ratio at the plateau. For the initial recombining situation of the last section, Fig. 3 shows that a value of k_r can be determined for $\tau_{\min}\leqslant t\leqslant\tau_{\max}$, with $\tau_{\max}\simeq10^{-5}$ s. The minimal time $\tau_{\min}$ corresponds to the necessary time to reach a quasi-steady-state (Figs. 2 and 3) and is denoted $\tau_{\rm QSS}$ in the following. For $t>\tau_{\max}$, ionization processes become significant and then the first term on the right-hand side of Eq. (13) is no longer negligible in comparison to the second one. Finally, Fig. 3 clearly shows that a quasi-steady-state condition has to be reached to determine k_r. In the case of an initial ionizing situation, the general characteristics of the results are the same.

Finally, to determine k_r, respectively k_i, we start from an initial recombining, respectively ionizing situation, and, stop the calculations when $|\dot{n}_e|$ and $|\dot{N}_1+\dot{N}_2+\dot{N}_3|$ agree to within 1%. Then we determine $\tau_{\rm QSS}$ and the value of k_r, respectively k_i, with the instantaneous values of $\dot{n}_e$, and n_e^3, respectively $n_e N_a$. The interest of this approach is the possibility to follow the temporal evolutions of populations and to determine also $\tau_{\rm QSS}$.

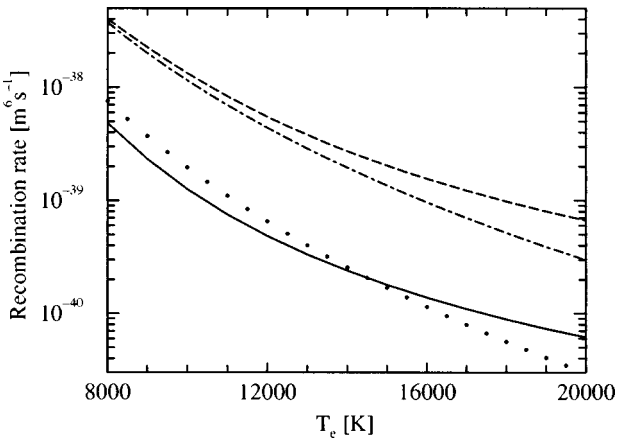

FIG. 4. Three-body recombination rate in an optically thick plasma. Solid line: our model. Dot-dashed line: Park's expression [9]. Dashed line: our atomic model and the cross sections derived by Gryzinski [22]. Dotted line: Three-body recombination rate of nitrogen [1].

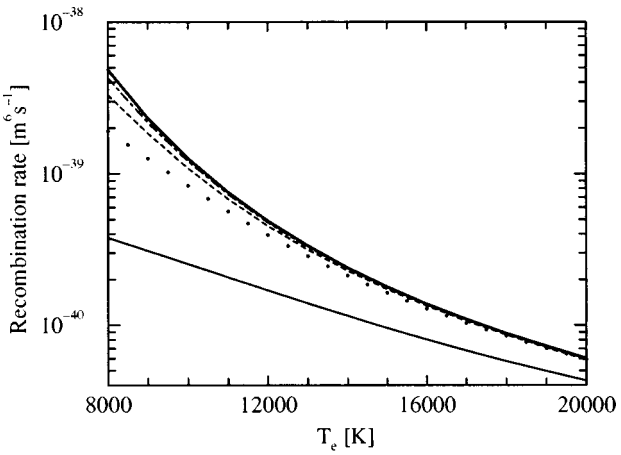

FIG. 5. Influence of the number of atomic levels on the derived recombination rate in optically thick cases. Thick solid line: our 40 level model. Thin solid line: 9 levels [4]. Dotted line: 15 levels. Dashed line: 20 levels. Dot-dashed line: 30 levels.

As already mentioned in paper I, ionization and recombination rate coefficients are not independent. Indeed, at the stationary state of the reaction $O^+ + 2e^- \leftrightarrow O + e^-$, the two terms on the right hand side of Eq. (13) have to balance to give $\dot{n}_e = 0$. Then, k_i can be derived from k_r by

$$k_i = k_r \frac{[n_e^{\text{stat}}]^2}{N_a^{\text{stat}}} = k_r K^{\text{stat}}. \tag{14}$$

We have checked that both methods gave the same results.

C. Determination of the effective three-body recombination rate coefficient

1. Optically thick cases

In order to represent an optically thick medium, in this section, all the escape factors in Eqs. (8) and (9) are set equal to zero. Then, as only elementary collisional processes are considered, the results of this section are denoted with the superscript C. As in nitrogen, in optically thick conditions, we have checked that the three-body recombination rate coefficient for oxygen depends only on the electron temperature (Fig. 4). The simplest best-fit curve for our computed result is

$$k_r^C = 1.32 \times 10^{-39} \left(\frac{T_e}{10^4} \right)^{-4.66} \text{ m}^6 \text{ s}^{-1} \tag{15}$$

for 8000 K$\leqslant T_e \leqslant$20 000 K. Park [9] assumed that the three-body recombination rate of oxygen is the same as that of nitrogen, derived for 4000 K$\leqslant T_e \leqslant$20 000 K in using for all levels the elementary rates derived by Gryzinski [22] for hydrogen

$$k_{r\text{Park}} = 1.15 \times 10^{-38} \left(\frac{T_e}{10^4} \right)^{-5.27} \text{ m}^6 \text{ s}^{-1}. \tag{16}$$

Figure 4 shows that, over the whole temperature range of this study, the value obtained with our model is on the average five times smaller than the one proposed by Park. With our method, we have also calculated the effective three-body recombination rate coefficient (denoted k_r^{H}) obtained when one uses for all levels the elementary rates derived by Gryzinski [22] for hydrogen. In this case, Fig. 4 shows that the value of k_r^{H} is close to the one proposed by Park. Cacciatore and Capitelli [5] proposed to modify the elementary rate coefficients derived by Gryzinski to take into account that low-lying levels of atomic oxygen are nonhydrogenic. That is, the Gryzinski values are multiplied by a factor 4 for the ground state. It is interesting to mention that this correction has no influence on the calculated value of k_r^{H} for atomic oxygen. Finally, in Fig. 4, the fitting law obtained in paper I for atomic nitrogen is represented. This law is given for 4000 K$\leqslant T_e \leqslant$12 000 K and, therefore should be handled with care for $T_e >$12 000 K. However, it is interesting to note that three-body recombination rates for oxygen and nitrogen remain close to each other for 8000 K$\leqslant T_e \leqslant$20 000 K.

2. Influence of the number of levels

Figure 5 shows the influence of the number of atomic levels on the calculated effective three-body recombination rate coefficient value in optically thick cases. As the number of atomic levels increases, the calculated recombination rate converges toward an upper limit. This figure puts forward clearly that the 9-level model proposed by Soon and Kunc [4] is unadapted to our temperature range and that it was necessary to consider a more sophisticated atomic model. Our forty level model appears to be a good compromise between the inaccuracy of atomic models for highly excited levels and the reliability of the effective rate coefficients derived in this study.

3. Optically thin cases

As in nitrogen, in optically thin cases, we have checked that the three-body recombination rate coefficient for oxygen depends only on the electron temperature and number density. First, neglecting radiative and dielectronic recombinations, Fig. 6 shows that spontaneous emission increases the value of the recombination rate (denoted, in this case, k_r^{CE}).

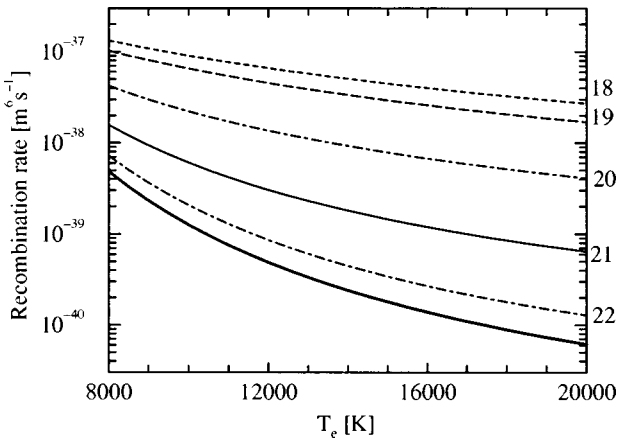

FIG. 6. Influence of spontaneous emission on the recombination rate in an optically thin plasma. Numbers at right denote x with $n_e = 10^x$ m^{-3}. The thick solid line corresponds to optically thick cases.

As expected, at high electron number densities, the recombination rate converges to the value obtained in optically thick cases. Conversely, for low electron number densities, k_r^{CE} tends toward an upper limit. If all the elementary processes of Sec. III are considered, Fig. 7 shows that the influence of radiative and dielectronic recombinations increases as n_e decreases. In this case, the recombination rate has no upper limit at low electron number densities. These results are in qualitative agreement with those obtained earlier by Taylor and Ali [2]. Figure 7 indicates that Park's expression [Eq. (16)], initially proposed for an optically thick case, corresponds to an optically thin plasma where 10^{20} m$^{-3} \leqslant n_e \leqslant 10^{21}$ m^{-3} and 8000 K$\leqslant T_e \leqslant$20 000 K.

In order to implement the results of this work in numerical studies on air plasma flows, simple analytical laws are required. In the general Eq. (9), radiative and dielectronic terms can be isolated, then Eq. (13) can be written as

$$\frac{dn_e}{dt} = \dot{n}_e = k_i n_e N_a - k_r^{\mathrm{CE}} n_e^3 - \alpha^R n_e^2, \tag{17}$$

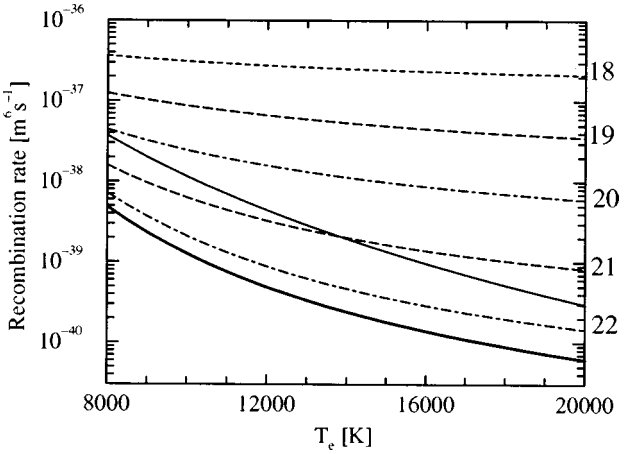

FIG. 7. Three-body recombination rate derived in taking into account all elementary processes, in an optically thin plasma. Numbers at right denote x with $n_e = 10^x$ m^{-3}. The thick solid line corresponds to optically thick cases. The thin solid line corresponds to Park's expression [9].

TABLE II. Parameters in the effective three-body recombination rate coefficient k_r^{CE} for different electron number densities.

n_e (m^{-3})	A (m^6 s^{-1} K^{-b})	b
10^{18}	7.27×10^{-31}	-1.73
10^{19}	4.29×10^{-30}	-1.95
10^{20}	2.58×10^{-28}	-2.51
10^{21}	3.19×10^{-25}	-3.43

where k_r^{CE} takes into account all the elementary collisional processes and spontaneous emission (Fig. 6), and

$$\alpha^R = \alpha^{\mathrm{RR}} + \alpha^{\mathrm{RD}}. \tag{18}$$

The total effective recombination rate k_r is therefore $k_r^{\mathrm{CE}} + \alpha^R/n_e$. This formulation is of great interest since α^{RR} [Eq. (7)] and α^{RD} [28] can be expressed analytically. Then, we fitted k_r^{CE} for different electron number densities to the following expression:

$$k_r^{\mathrm{CE}} = A T_e^b \ \ \mathrm{m^6\ s^{-1}} \tag{19}$$

for 8000 K$\leqslant T_e \leqslant$20 000 K. The coefficients A and b are given in Table II. The discrepancy between the total recombination rate value calculated with the analytical expressions [Eqs. (19) and (18)] and the one determined directly and represented on Fig. 7 remains within a factor of 2.

D. Determination of the effective ionization rate coefficient

1. Optically thick cases

In optically thick cases, the results obtained for different initial ionizing conditions indicate that the effective ionization rate coefficient (denoted k_i^C) depends only on the electron temperature. This can be simply derived from Eq. (14), since in this case, k_r^C depends only on T_e and the stationary state of the reaction $\mathrm{O^+ + e^- \leftrightarrow O + 2e^-}$ corresponds to a Saha equilibrium, therefore $K^{\mathrm{stat}} = K^{\mathrm{Saha}}(T_e)$. We have fitted the equilibrium constant to the following expression:

$$\ln(K^{\mathrm{stat}}) = \sum_{i=0}^{5} A_i Z^i, \tag{20}$$

where $Z = \ln(10^4/T_e)$, for 8000 K$\leqslant T_e \leqslant$20 000 K. For a Saha equilibrium, the coefficients A_i are given in Table III.

Figure 8 compares the value of k_i^C obtained in our study with three other values often used in high-temperature air kinetic schemes, but whose accuracy is unknown: (i) The effective ionization rate coefficient proposed by Losev *et al.* [11], which is derived from the ionization cross section from the ground state measured by Smith *et al.* [30],

$$k_{i\mathrm{Losev}} = 8.64\times10^{-18} T_e^{0.68} \exp\left(\frac{-157980}{T_e}\right) \ \ \mathrm{m^3\ s^{-1}}; \tag{21}$$

(ii) the value proposed by Gupta *et al.* [10]:

$$k_{i\mathrm{Gupta}} = 59.8 T_e^{-2.91} \exp\left(\frac{-158120}{T_e}\right) \ \ \mathrm{m^3\ s^{-1}}; \tag{22}$$

TABLE III. Parameters in K^{Saha} and in the equilibrium constant K^{stat} for different total particle number densities.

N_t (m^{-3})	A_0	A_1	A_2	A_3	A_4	A_5
10^{17}	30.5304	−34.0190	−23.6944	6.18581	−0.916160	−17.5735
10^{18}	32.8715	−33.1659	−22.8399	7.45801	5.02374	−11.8446
10^{19}	35.0493	−31.4172	−24.8850	−0.795804	17.3478	11.0059
10^{20}	36.6971	−27.7121	−6.36738	−49.7549	−187.362	−149.453
10^{21}	38.6205	−35.9083	6.47223	62.7877	−35.6484	−97.7333
10^{22}	41.9019	−45.7554	−37.4442	166.309	443.193	298.333
10^{23}	45.2287	−31.9500	−57.7671	−69.9729	−17.6998	19.8520
K^{Saha}	47.0661	−17.1846	−7.99356	−2.64241	−0.579718	0.182226

(iii) the value proposed by Park [9]:

$$k_{i\text{Park}} = 6478.4 T_e^{-3.78} \exp\left(\frac{-158620}{T_e}\right) \ \text{m}^3\,\text{s}^{-1}. \quad (23)$$

First of all, we note that there are strong discrepancies between the different models. As expected, the value obtained with our model is greater than the one proposed by Losev *et al.* since the latter takes into account only the ionization process from the ground state. Figure 8 shows that the value proposed by Gupta *et al.* is overestimated by more than one order of magnitude. In fact, the value of k_i^C obtained with our model turns out to be in close agreement with the one proposed by Park. This result seems to be in disagreement with the discrepancy observed on Fig. 4 between our value of the three-body recombination rate in optically thick cases (k_r^C) and the one proposed by Park ($k_{r\text{Park}}$). In fact, we have noted that the ionization and recombination rate coefficients proposed by Park in optically thick cases are not related by the Saha equilibrium constant. That is, $k_{r\text{Park}} K^{\text{Saha}}$ is on the average 4.7 times greater than $k_{i\text{Park}}$, which is also the average discrepancy observed on Fig. 4 between k_r^C and $k_{r\text{Park}}$.

2. Optically thin cases

In optically thin cases, K^{stat} depends on T_e but also on densities. As in nitrogen, to characterize the stationary state, the most significant density is the total particle density N_t. First, neglecting radiative and dielectronic recombination processes, Fig. 9 shows the equilibrium constant for different values of N_t. As expected, as the density increases, collisional processes become more efficient than radiative ones, and then the equilibrium constant converges toward the Saha equilibrium constant, all the faster since the electron temperature is high. At low density, the equilibrium constant tends toward a lower limit. When radiative and dielectronic recombination processes are taken into account, Fig. 10 shows that this lower limit disappears. As Soon and Kunc [4] considered more accurately the reabsorption of the emitted radiation, a direct comparison with their results at the stationary state is impossible. However, a qualitative agreement is observed. Finally, to implement our results in flow codes, we have fitted K^{stat} for different values of N_t to the expression of Eq. (20) for 8000 K$\leqslant T_e \leqslant$20 000 K. The coefficients A_i are given in Table III. The discrepancy between the ionization rate coefficient value calculated with the analytical expression [Eq. (20)] and the one determined directly and represented on Fig. 10 remains within a factor of 2.

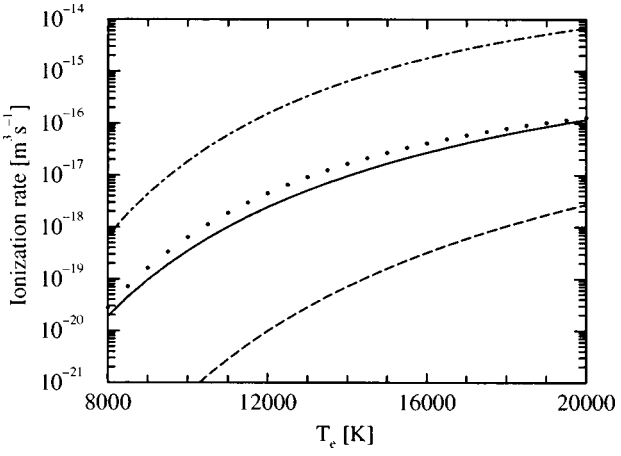

FIG. 8. Ionization rate coefficient in optically thick cases. Solid line: our model. Dotted line: Park's expression [9]. Dot-dashed line: Gupta *et al.*'s expression [10]. Dashed line: Losev *et al.*'s expression [11].

E. Study of the QSS relaxation time

In the preceding sections, we have put forward that effective three-body recombination and ionization rate coefficients exist only when the system is in a quasi-steady-state. Therefore, before implementing these rate coefficients in

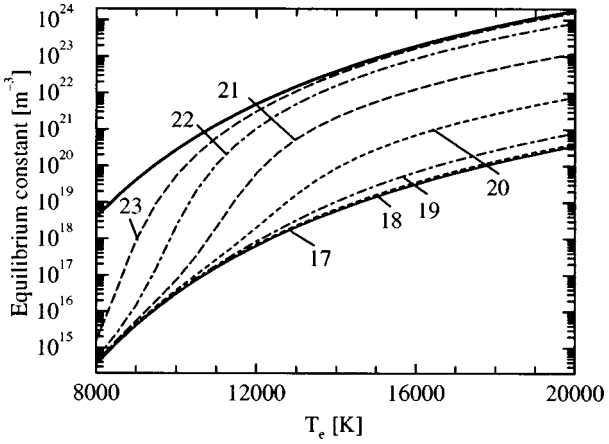

FIG. 9. Influence of spontaneous emission on the equilibrium constant in an optically thin plasma. Numbers denote x with $N_t = 10^x$ m^{-3}. The thick solid line corresponds to the Saha value.

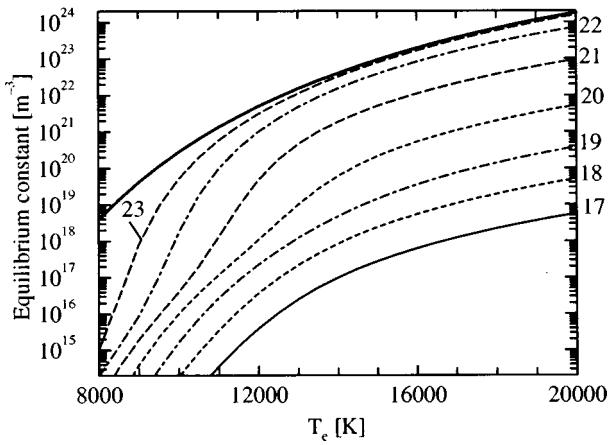

FIG. 10. Equilibrium constant when all elementary processes are taken into account. Numbers denote x with $N_t = 10^x$ m^{-3}. The thick solid line corresponds to the Saha value.

flow codes, one has to check the validity of the QSS hypothesis [Eq. (11)]. The time-dependent approach used in this paper allows us to determine the relaxation time necessary to reach a quasi-steady-state, starting at $t = 0$ s from a given initial condition.

1. Optically thick cases

For optically thick cases, the results obtained for different initial conditions (either ionizing or recombining) indicate that the quasi-steady-state relaxation time (denoted $\tau^C_{\rm QSS}$) depends only on the electron temperature and electron number density but not on the initial distribution on the atomic levels. Figure 11 shows that $\tau^C_{\rm QSS}$ depends only weakly on T_e but increases as n_e decreases. For $n_e = 10^{19}$ m^{-3}, the relaxation time derived in using Gryzinski's cross sections for all levels is also represented. The latter is one order magnitude shorter than the one obtained with our model. It is interesting to note that relaxation times obtained in oxygen are very close to those calculated in nitrogen. Therefore, as in nitrogen, we conclude that the effective ionization and recombination rate coefficients determined in this paper are adapted to study optically thick plasma flows, where the characteristic flow time is about 10^{-6} s, only if $n_e \geqslant 10^{20}$ m^{-3}. For lower electron number densities or shorter flow times, it is necessary to consider one conservation equation for each atomic level i of the oxygen atom.

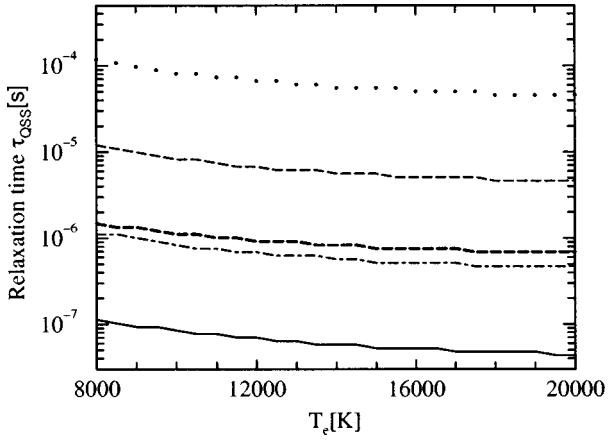

FIG. 11. Relaxation time in optically thick cases. Thin lines correspond to different electron number densities. Thin dotted line: $n_e = 10^{18}$ m^{-3}. Thin dashed line: $n_e = 10^{19}$ m^{-3}. Thin dot-dashed line: $n_e = 10^{20}$ m^{-3}. Thin solid line: $n_e = 10^{21}$ m^{-3}. The thick dashed line represents the results obtained for $n_e = 10^{19}$ m^{-3} in using the cross sections derived by Gryzinski [22] for hydrogen.

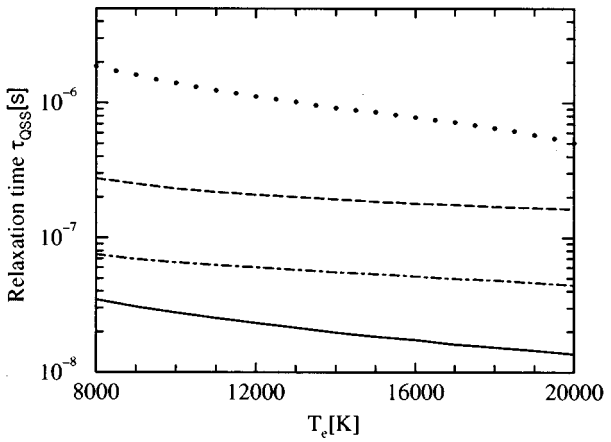

FIG. 12. Relaxation time in optically thin cases with at $t = 0$ s, $b_i = N_i / N_i^* = 1$, for a given electron number density. Dotted line: $n_e = 10^{18}$ m^{-3}. Dashed line: $n_e = 10^{19}$ m^{-3}. Dot-dashed line: $n_e = 10^{20}$ m^{-3}. Solid line: $n_e = 10^{21}$ m^{-3}.

2. Optically thin cases

In an optically thin plasma, the relaxation time depends on densities and T_e but also on the initial distribution on atomic levels. Therefore, it is more difficult to derive general results. However, we have noted that for initial recombining conditions with at $t = 0$ s $b_i = N_i / N_i^* \leqslant 1$ (where N_i^* is the Saha density of level i) for a given electron number density, the QSS relaxation time depends only on n_e and T_e. In these cases, Fig. 12 shows that the QSS relaxation time depends weakly on T_e and increases as n_e decreases. In comparison to an optically thick case, we note that relaxation times are on the average one order of magnitude shorter.

VI. CONCLUSIONS

In this paper, we have determined the effective ionization and three-body recombination rate coefficients of oxygen in a plasma where 10^{18} m$^{-3} \leqslant n_e \leqslant 10^{21}$ m^{-3} and 8000 K$\leqslant T_e \leqslant$20 000 K. In optically thick cases, we propose an analytical expression of $k_r^C(T_e)$ to be implemented in flow codes [Eq. (15)]. This rate coefficient value is on the average five times smaller than the one given by Park [9]. In optically thick cases, the ionization rate coefficient is simply $k_i^C(T_e) = k_r^C(T_e) K^{\rm Saha}(T_e)$ where $K^{\rm Saha}$ is the Saha equilibrium constant. This ionization rate coefficient is in close agreement with the one proposed by Park [9] but is more than one order of magnitude greater, respectively less, than the rate coefficient proposed by Losev *et al.* [11], respectively, Gupta *et al.* [10]. In optically thin cases, radiative processes enhance recombination and then increase the effective recombination rate coefficient. As in nitrogen, we have shown that the total recombination rate coefficient of oxygen k_r could be written as $k_r^{\rm CE} + \alpha^R / n_e$, where $k_r^{\rm CE}$ takes into account all the elementary collisional processes and spontaneous emission and α^R

dielectronic and radiative recombination processes. In order to implement these new results in plasma flow codes, simple analytical expressions for k_r^{CE} [see Eq. (19) and Table II] and α^R [see Eq. (7) and [28]] are proposed. The ionization rate coefficient is related to k_r by the equilibrium constant K^{stat} [Eq. (14)]. In optically thin cases K^{stat} and therefore k_i depend on T_e and on the total density N_t. To implement these results in plasma flow codes, fitting laws are proposed for K^{stat} [see Eq. (20) and Table III]. The time-dependent approach used in this study has clearly put forward the necessity that the system be in a quasi-steady-state to derive meaningful rate coefficients. This has led us to study more precisely the relaxation time τ_{QSS} necessary to reach a quasi-steady-state. In optically thick cases, for recombining or ionizing plasmas τ_{QSS} depends only on T_e and n_e. It is interesting to point out that τ_{QSS} strongly increases as n_e decreases. Therefore, the effective ionization k_i^C and recombination k_r^C rate coefficients derived in this study may be implemented in the computation of supersonic plasma flow codes, where the characteristic flow time is about 10^{-6} s only for an electron number density higher than 10^{20} m^{-3}. In optically thin cases, it is more difficult to derive general results since τ_{QSS} depends on T_e and densities and on the initial distribution on atomic levels.

In this study, the treatment of radiation has been reduced to optically thin or thick cases. It would be interesting to take into account a more accurate modeling of radiation escape factors in order to study more precisely the influence of the reabsorption of radiation. However, this effect will not change the general characteristics of the results obtained in this paper.

Finally, one should mention the question of the influence of the accuracy of the cross sections and Einstein coefficients on the results. Currently, no complete set of precalculated cross sections is available for oxygen. Therefore, for low atomic levels, we have used the Vainshtein formalism, which is certainly more adapted than hydrogenic models retained in earlier studies. It would be interesting to compare our results with those obtained with more accurate quantum mechanical methods such as close-coupling and R-matrix methods. But these methods are computer intensive, and have been completed, up to now, only for a few systems [31].

[1] A. Bourdon and P. Vervisch, Phys. Rev. E **54**, 1888 (1996).
[2] R. D. Taylor and A. W. Ali, J. Quant. Spectrosc. Radiat. Transf. **36**, 373 (1986).
[3] A. M. Gomès, A. Essoltani, and J. Bacri, J. Quant. Spectrosc. Radiat. Transf. **43**, 471 (1990).
[4] W. H. Soon and J. A. Kunc, Phys. Rev. A **41**, 825 (1990).
[5] M. Cacciatore and M. Capitelli, J. Quant. Spectrosc. Radiat. Transf. **16**, 325 (1976).
[6] J. P. Doering, Geophys. Res. Lett. **19**, 449 (1992).
[7] E. Biémont and C. J. Zeippen, Astron. Astrophys. **265**, 850 (1992).
[8] A. K. Bhatia and S. O. Kastner, Astrophys. J., Suppl. Ser. **96**, 325 (1995).
[9] C. Park, *Non-Equilibrium Hypersonic Aerothermodynamics* (Wiley, New York, 1990).
[10] R. N. Gupta, J. M. Yos, R. A. Thompson, and K. P. Lee, NASA Technical Report No. RP1232, 1990.
[11] S. A. Losev, V. N. Makarov, M. J. Pogosbekyan, and O. P. Shatalov, in *Proceedings of the American Institute of Aeronautics and Astronautics, 6th AIAA/ASME Joint Thermophysics and Heat Transfer Conference* (American Institute of Aeronautics and Astronautics, Washington, DC, 1994).
[12] C. E. Moore, in *Tables of Spectra of Hydrogen, Carbon, Nitrogen, and Oxygen Atoms and Ions*, edited by J. W. Gallagher (CRC Press, Boca Raton, FL, 1993), pp. 203–209.
[13] W. H. Soon and J. A. Kunc, Phys. Rev. A **43**, 723 (1991).
[14] J. P. Doering and E. E. Gulcicek, J. Geophys. Res. **94**, 2733 (1989).
[15] J. P. Doering and E. E. Gulcicek, J. Geophys. Res. **94**, 1541 (1989).
[16] E. E. Gulcicek, J. P. Doering, and S. O. Vaughan, J. Geophys. Res. **93**, 5885 (1988).
[17] E. E. Gulcicek and J. P. Doering, J. Geophys. Res. **93**, 5879 (1988).
[18] R. R. Laher and F. R. Gilmore, J. Phys. Chem. Ref. Data **19**, 277 (1990).
[19] L. D. Thomas and R. K. Nesbet, Phys. Rev. A **11**, 170 (1975).
[20] R. J. Henry, P. G. Burke and A. L. Sinfailam, Phys. Rev. **178**, 218 (1969).
[21] I. I. Sobelman, L. A. Vainshtein, and E. A. Yukov, *Excitation of Atoms and Broadening of Spectral Lines* (Springer-Verlag, New York, 1981).
[22] M. Gryzinski, Phys. Rev. A **138**, 322 (1965).
[23] M. Gryzinski and J. A. Kunc, J. Phys. B **19**, 2479 (1986).
[24] J. R. Fuhr and W. L. Wiese, in *CRC Handbook of Chemistry and Physics*, edited by D. R. Lide (CRC Press, Boca Raton, FL, 1990), pp. 128–179.
[25] S. S. Tayal and R. J. W. Henry, Phys. Rev. A **39**, 4531 (1989).
[26] J. P. Doering, E. E. Gulcicek, and S. O. Vaughan, J. Geophys. Res. **90**, 5279 (1985).
[27] D. A. Verner, E. M. Verner, and G. J. Ferland, At. Data Nucl. Data Tables **64**, 1 (1996).
[28] H. Nussbaumer and P. J. Storey, Astron. Astrophys. **126**, 75 (1983).
[29] A. C. Hindmarsh, ACM Signum Newslett. **15**, 10 (1980).
[30] A. C. Smith, E. Caplinger, R. H. Neynaber, E. W. Rothe, and S. M. Trujillo, Phys. Rev. **127**, 1647 (1962).
[31] A. K. Pradhan, in *Atomic Processes in Plasmas*, edited by A. Hauer and A. L. Mertf (Academic, New York, 1988).